E3S Web of Conferences **464**, 02008 (2023) https://doi.org/10.1051/e3sconf/202346402008
2nd ICDMM 2023

Study of the sub-surface geological condition of the Sibalaya flow liquefaction using seismic refraction method

Putu Pradnya Andika[1*], *Adrin* Tohari[2], and *Dadan* Dani Wardhana[2]

[1]Geophysical Engineering Departement, Institut Teknologi Sumatera, Lampung, Indonesia
[2]Research Center for Geological Disaster, National Research and Innovation Agency, Bandung, Indonesia

Abstract. Understanding the occurrence of flow liquefaction requires knowledge of the sub-surface condition controlling its occurrence. This paper presents the results of seismic refraction surveys conducted to evaluate the sub-surface geological condition in the Sibalaya flow liquefaction area. From the interpretation of the seismic refraction model, an inclined boundary presents between the near-surface sediment layers. Further examinations of the SRT images demonstrate the existence of localized basinal structures in the rock layer with the highest P-wave velocity. The basinal structure may be associated with a hidden normal fault system of horst-graben structures. Thus, this study indicates that such a complex sub-surface geological structure also contributed to the Sibalaya flow liquefaction occurrence.

1 Introduction

A big earthquake of Mw 7.5 that struck the northern part of the Central Sulawesi region on September 28th, 2018 not only triggered a series of tsunami waves in the coastal areas but also flow liquefaction phenomena in some residential areas in Sigi Regency and Palu City. Such a liquefaction event claimed hundreds of lives and contributed to significant economic losses.

One flow liquefaction phenomenon occurred in the Sibalaya Village in Sigi Regency, about 35 km south of Palu City (Figure 1). The easternmost boundary of the Sibalaya liquefaction area is limited by an irrigation canal. The liquefaction destroyed about 150 houses and hundreds of hectares of rice fields and was probably caused by the breach of the irrigation canal [1].

A previous study has focused on establishing the hypothesized mechanism of the Sibalaya flow liquefaction based on morphological features and eyewitness accounts [1, 2] and trenching data [3]. However, none has been attempted to clarify the sub-surface factor causing the occurrence of flow liquefaction. Using a seismic refraction survey method, [4] studied a flow liquefaction phenomenon in Lolu Village, located a few kilometers from the Palu Koro Fault. They found the existence of localized horst and graben, assumably associated with the pull-apart basin in the Lolu liquefaction area. Their study suggests that complex sub-surface geological structures may contribute to the occurrence of a flow liquefaction.

Considering that the location of the Sibalaya liquefaction is about a few kilometers east of the 2018 Palu Koro Fault rupture, it is interesting to understand the factors controlling the occurrence of liquefaction in this location. Referring to [2], a series of geophysical explorations (electrical resistivity and/ or seismic) was recommended to produce the subsurface profile to understand the heterogeneity at the Sibalaya site. Meanwhile, [5] speculated that the flow liquefaction phenomena were apt to be caused by the sufficient supply of groundwater to the liquefied mass through the fractures formed by the movement of hidden faults. Thus, knowledge of sub-surface geological structure is important to clarify the cause of the Sibalaya flow liquefaction.

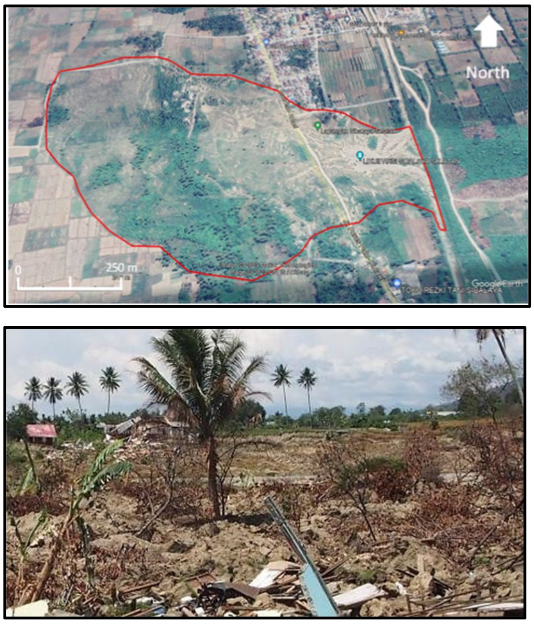

Fig. 1. The areal photograph of the Sibalaya flow liquefaction (top) and destroyed houses (bottom).

* Corresponding author : putu.andika@tg.itera.ac.id

In this paper, the results of seismic refraction surveys in the Sibalaya flow liquefaction site are presented, aiming to evaluate the sub-surface geological condition controlling the flow liquefaction occurrence. The objectives of this survey were to (1) identify the geometry of rock layer boundaries and (2) interpret the sub-surface geological structure based on the variation of the P-wave velocities.

2 Surficial geology of Palu Valley

According to [6], the geomorphology of the Palu Valley region can be divided into two classes: structural denudational and fluvial origins. The former is composed mainly of gently rolling hilly topography and mountainous ridges with a slope inclination of more than 5%, extending to the north and east Palu Valley regions. In contrast, the latter consists of alluvial fans, flood plains, and river beds with a slope inclination of not more than 5%, and dominates the center part of Palu Valley. According to post-earthquake field observations, all flow liquefaction events took place in the fluvial geomorphological origin.

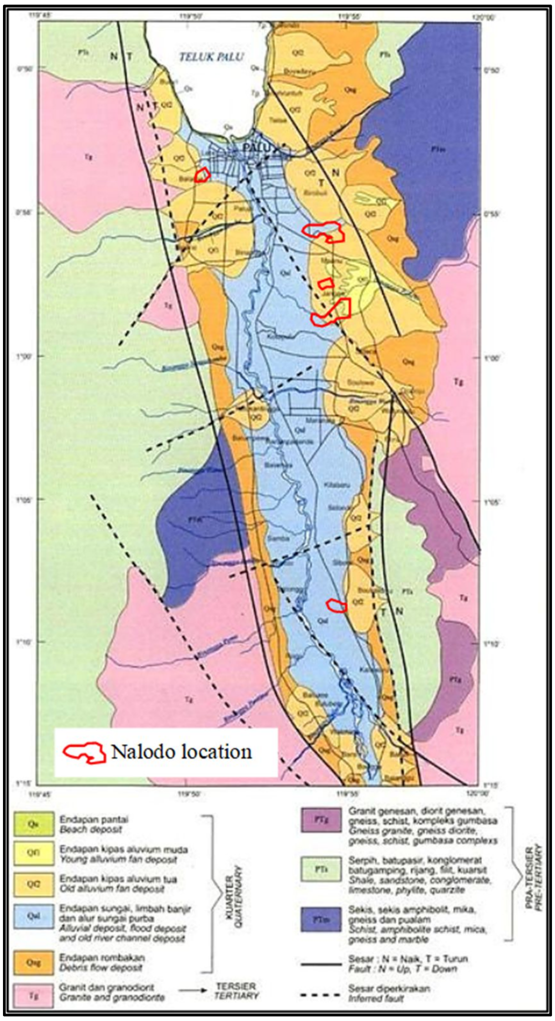

Fig. 2. Surficial geological map of Palu Valley (modified from [1]).

As shown in Figure 2, the Palu Valley area is, geologically, made up of the Pre-Tertiary rock formation and Quaternary rocks. The Pre-Tertiary rocks consist of metamorphic rocks of the Palu Complex and Gumbasa Complex and sedimentary rocks of the Tinombo Formation, and Celebes Molasses. Meanwhile, the Quaternary rocks comprise alluvium and coastal deposits, almost covering the coastal area. Some intrusive rocks of different generations are also present in the area. Towards the Palu Bay area, alluvial and coastal deposits overlap the older rock formations, Celebes Molasses and Metamorphic Complex. Alluvial deposits, without coastal deposits, can also be unearthed a few tens of km south of the Palu Bay area, overlying the Celebes Molasses.

The main geological structure in the Palu Valley area is the Palu-Koro Fault, an active strike-slip fault trending to NNW–SSE with a left-lateral movement [7-11]. This active fault is noticeable within the valley and cuts across the lower section of old alluvial fans. It is distinguished by the intra-basin ridge in the slightly uplifted ground surface from the adjacent surfaces [12]. The earthquake event on 28 September 2018 with a magnitude Mw of 7.5 unveiled the main fault rupture, detectable from Palu Bay to Sigi Regency [11, 13]. A maximum slip of 6±0.5 m was produced within Palu City, with an average slip of up to 4.7 m in the southern and northern parts of the city [13].

3 Methods

3.1 Data acquisition

To accomplish the objectives of the study, the seismic refraction surveys were performed within the flow liquefaction area in Sibalaya village using the 24-channel seismic system, the McSEIS-SX48, in conjunction with 28 Hz geophones, for data acquisition. To fully capture the liquefaction area, the survey comprised one survey line in the East-West direction, and two survey lines in the North-South direction, as shown in Figure 3. In total, each survey line is 115 meters long with a geophone spacing of 5 meters and 5 shoot points at 27.5 meters intervals as shown in Figure 4. Table 1 summarizes the geophone coordinate and length information for each line study.

Fig. 3. Design of the SRT survey lines drawn in a satellite image of the area taken in 2022.

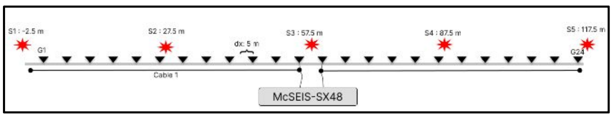

Fig. 4. The 24-geophones configuration and shoot point locations in the SRT survey line.

https://doi.org/10.1051/e3sconf/202346402008

Table 1. Coordinate the position and profile length of the SRT survey lines

Line Survey	1st Geophone		24th Geophone		Total Length (m)
	UTM X	UTM Y	UTM X	UTM Y	
Line S1	825390	9873072	825387	9872961	115
Line S2	825338	9873017	825451	9873003	115
Line S3	825372	9873076	825361	9872965	115

3.2 Data processing

To process the seismic refraction data, the SeisImager software, which includes Seisrefa and Pickwin functionality, was used. Figure 5 depicts a schematic illustration of this procedure. We were able to choose the initial arrivals from the seismic data for each shot along the profiles using this program. Following that, a 2D velocity model was created using the tomographic inverse method.

A gradual velocity model was used as a starting point in the early phases. Using an iterative least squares inversion approach, we modified the model's parameters until the stop criteria were fulfilled with an RMSE not more than 2 milliseconds or by a maximum number of iterations. This methodical technique assured the quality and dependability of the created 2D velocity model.

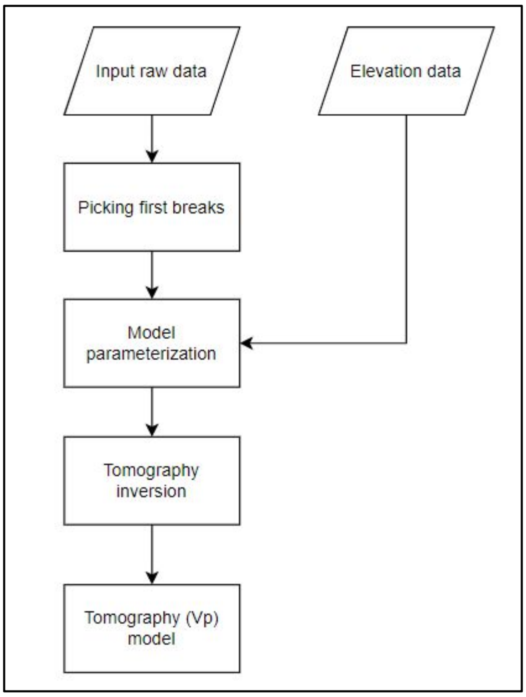

Fig. 5. General procedure for processing data using SeisImager software.

4 Result and discussion

4.1 Variation of P-wave velocity

Figures 6 to 8 show the refraction tomography images that were acquired. The seismic refraction tomography (SRT) images show a relatively low P-wave velocity in the shallow subsurface area, contrasting with an increase in velocity at increasing depths across all examined profiles. A four-layered subsurface structure may be seen in individual SRT models. The top layer has a velocity of 300-900 m/s and a thickness of about 7 meters. The second layer is characterized by P-wave velocities ranging from 900-1500 m/s and has a thickness variation of 5-7.5 meters. The third rock layer, about 5 to 17.5 m thick, is distinguished by velocities between 1500 and 2000 m/s. The fourth layer is typified by velocities of higher than 2000 m/s. It is clear that the boundary between layers #1 and #2 forms an inclined plane parallel to the flow direction. Thus, the sub-surface topographical factor is attributable to the flow liquefaction occurrences in this area. Such a sub-surface factor is also observed in Balaroa, and Petobo [14] as well as in Lolu areas [4].

4.2 Seismic refraction tomography model

A graben structure is seen in the middle section of Line-S1 shown in Figure 6(a), demonstrating that Line-S1 is contained within the zone affected by liquefaction. Figure 6(b) depicts the explanation of this seismic tomographic model, which shows the development of a horst and graben configuration in the fourth rock layer. This model, in particular, clearly elucidates the emergence of a pull-apart basin structure.

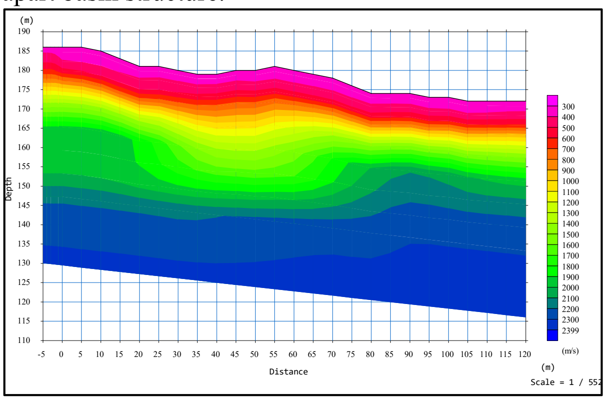

(a) SRT model

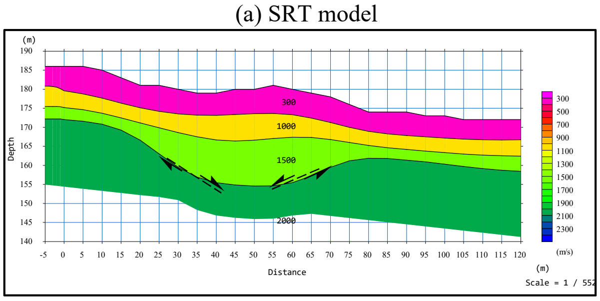

(b) The sub-surface structure interpretation

Fig. 6. SRT model and its interpretation of the sub-surface structure for Line S1.

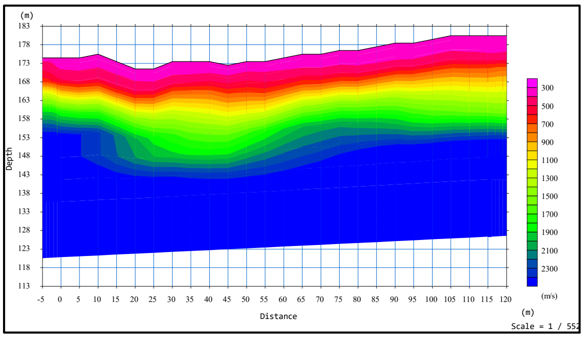

(a) SRT model

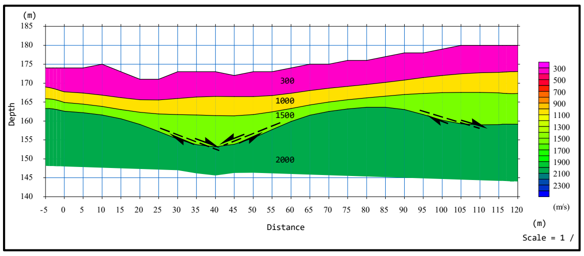

(b) The sub-surface structure interpretation

Fig. 7. SRT model and its interpretation of the sub-surface structure for Line S2.

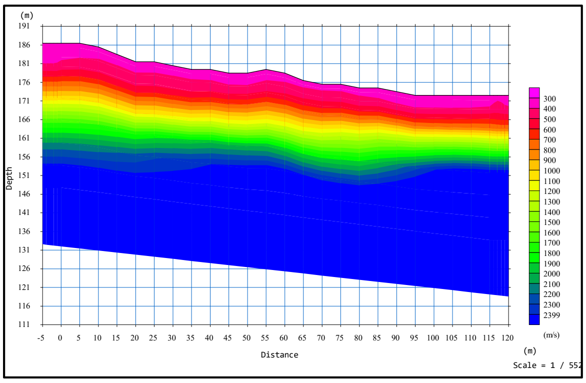

(a) SRT model

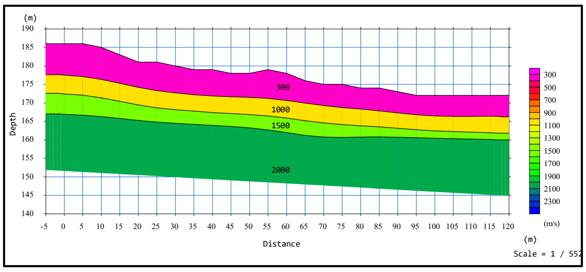

(b) The sub-surface structure interpretation

Fig. 8. SRT model and its interpretation of the sub-surface structure for Line S3.

According to Figure 7(a), the thickness of the third layer in Line S2 varies about 8 meters in the east, increases up to 15 meters in the middle of the profile, and then decreases up to 2.5 meters in the east. As a result, the seismic tomography model delineates the presence of a sub-surface basin shape under the liquefaction-affected region, which might be connected to a localized graben structure in the fourth rock layer. Figure 7(b) depicts the graben structure as an important component of a regionally constrained pull-apart basin phenomena.

Meanwhile, the SRT model for Line S3 is shown in Figure 8(a). The thickness of the first and second layers seems to be constant. Meanwhile, the third layer is relatively thicker in the north and becomes thinner towards the southern part, with thickness variation from 2.5 to 5 meters. Although the presence of horst and graben in the layered model is not visible in Figure 8(b), a shallow basin exists locally in the southern part of the survey line.

4.3 Implication to flow liquefaction mechanism

Many recent works have attempted to clarify the mechanism of earthquake-induced flow liquefaction phenomena in Palu and Sigiy Regency. The water interlayer hypothesis has been used to explain the mechanism of flow liquefaction [3-5]. However, this water interlayer concept alone can not explain the mechanism governing the Sibalaya flow liquefaction [3, 5]. As mentioned previously, the movement of a buried fault could contribute to the abundant supply of groundwater for a long-distance flow slide to occur [5]. All the SRT images exhibited the presence of localized pull-apart basins associated with a complex normal fault system in the liquefaction area. Some eyewitnesses described the sequence of earthquake shaking as an initial period of intense horizontal motion followed by a strong vertical motion and a sudden vertical drop at the end of the earthquake before the flow liquefaction occurred [1-3]. The vertical ground shaking was not recorded by the accelerometer in Balaroa [3], suggesting that this ground motion may be attributed to the movement of the local normal faults in the area. This fault movement then ruptured the confined aquifers and consequently increased the groundwater table causing the flow liquefaction to occur. The water was observed to overflow from a well located in the vicinity of the liquefaction area for two days and then, the well began to dry up in the next two weeks [3]. This evidence indicates an abundant supply of groundwater to the liquefiable layer through the cracks developed by the movement of the local faults.

5 Conclusions

Based on P-wave velocity distribution, the seismic refraction tomography (SRT) method used in this work successfully captures the sub-surface structures. The output of a tomographic image reveals the thickness of the layer model as well as the depth and undulation of the bedrock. According to the interpretation of the SRT models, the presence of a pull-apart basin associated with a complex normal fault system is more apparent in the middle area to the northern part of the study area. Such a sub-surface geological structure is likely to contribute to the flow liquefaction in the study area by facilitating the groundwater level to increase through the crack developed by the movement of this local fault system during the earthquake; the abundant supply of groundwater saturated the liquefiable soil layer. As the depth of the ruptured aquifer is still unknown, thus, further study using other geophysical exploration methods is needed to develop the sub-surface model required to clarify the mechanism of the Sibalaya flow liquefaction.

References

1. H.B. Mason, A.P Gallant, D. Hutabarat, J. Montgomery, A.N. Reed, J. Wartman, *et al*., Geotechnical Reconnaissance: The 28 September 2018 M7.5 Palu-Donggala, Indonesia Earthquake. Report No. GEER-061. Geotechnical Extreme Events Reconnaissance Association, Atlanta, Georgia, USA. 10.18118/G63376 (2019)
2. A.P. Gallant, J. Montgomery, H.B Mason, *et al*., Landslides **17**,1925 (2020)
3. M. Okamura, K. Ono, A. Arsyad, U.S. Minaka, S. Nurdin, Soil and Found. **60**, 1050 (2020)
4. P.P Andika, A. Tohari, T. Yudistira, E. Soebowo, J. Arifin, IOP Conf. Series: Earth and Environmental Science **1173**, 012029 (2023)
5. T. Kiyota, H. Furuichi, R.F. Hidayat, et al., Soils and Foundations **60**, 722 (2020)
6. R.A. van Zuidam, Aerial photo interpretation terrain analysis and geomorphology mapping, Smits Publisher, The Haque, Netherlands, 442 p (1985)
7. J.A. Katili, Geol Rundsch. **59**, 581 (1970)
8. H.D. Tjia, Bull. Geol. Soc. Malaysia **10**, 73 (1978)
9. O. Bellier, M. Sébrier, D. Seward, T. Beaudouin, M. Villeneuve, E. Putranto, Tectonophys. **413**, 201 (2006)
10. M.R. Daryono, Paleoseismologi Tropis Indonesia (Dengan Studi Kasus di Sesar Sumatra, Sesar Palukoro-Matano, dan Sesar Lembang). Dissertation Doctoral Program. Institut Teknologi Bandung (2016). Unpublished (*in Indonesian*)
11. I.M. Watkinson, R. Hall, Fault systems of the eastern Indonesian triple junction: evaluation of Quaternary activity and implications for seismic hazards Geohazards in Indonesia, in Earth Science for Disaster Risk Reduction. editor / P. Cummins; I. Meilano, Geol. Soc. London 441, **71** (2017)
12. A. Patria, P. S. Putra, Geosci. Lett. **7**, 1 (2020)
13. A.I. Abdullah, Abdullah, J. Phys.: Conference Series, **1434**, 012009 (2020)
14. A. Tohari, D.D. Wardhana, M. Hanif, K. Koizumi, E3S Web of Conferences **331**, 03002 (2021)